ISSN (Print) : 2320 – 3765
ISSN (Online): 2278 – 8875

International Journal of Advanced Research in Electrical, Electronics and Instrumentation Engineering

(An ISO 3297: 2007 Certified Organization)

Website: www.ijareeie.com

Vol. 6, Issue 4, April 2017

Design of A Novel Transformerless Hybrid Series Active Filter for Power Quality Improvement fed BLDC Drive

R.Ravindra Naik

Research Scholar, Department of Electrical & Electronics Engineering, QIS College of Engineering & Technology, Ongole, Andhra Pradesh, India

ABSTRACT: Transformers less hybrid series active filter for improve the power quality in single-phase systems with critical loads. The control strategy is designed to prevent current harmonic distortions of nonlinear loads to flow into the utility and corrects the power factor. This filter implemented in industries While protecting sensitive loads from voltage disturbances, sags, and swells initiated by the power system, ridded of the series transformer. This concept assists the energy management and power quality issues related to electric transportation and focuses on improving electric vehicle load connection to the grid. This hybrid topology allowing the harmonic isolation and compensation of voltage distortions could absorb or inject the auxiliary power to the grid. This concept can be extended by adding a BLDC drive load and going study the input response by using compensation and without compensation. The simulation results are presented by using Matlab/simulink platform.

KEYWORDS: Current harmonics, electric vehicle, hybrid series active filter (HSeAF), power quality, real-time control

I. INTRODUCTION

The forecast of future Smart Grids associated with electric vehicle charging stations has created a serious concern on all aspects of power quality of the power system; while widespread electric vehicle battery charging units [1], have detrimental effects on power distribution system harmonic voltage levels [3]. On the other hand, the growth of harmonics fed from nonlinear loads like electric vehicle propulsion battery chargers [4], which indeed have detrimental impacts on the power system and affect plant equipment, should be considered in the development of modern grids. Likewise, the increased rms and peak value of the distorted current waveforms increase heating and losses and cause the failure of the electrical equipment. Such phenomenon effectively reduces system efficiency and should have properly been addressed [6].

Moreover, to protect the point of common coupling (PCC) from voltage distortions, using a dynamic voltage restorer (DVR) function is advised. A solution is to reduce the pollution of power electronics-based loads directly at their source. Although several attempts are made for a specific case study, a generic solution is to be explored. There exist two types of active power devices to overcome the described power quality issues. The first category are series active filters (SeAFs), including hybrid-type ones. They were developed to eliminate current harmonics produced by nonlinear load from the power system. SeAFs are less scattered than the shunt type of active filters [8], [9]. The advantage of the SeAF compared to the shunt type is the inferior rating of the compensator versus the load nominal rating [10]. However, the complexity of the configuration and necessity of an isolation series transformer had decelerated their industrial application in the distribution system. The second category was developed in concern of addressing voltage issues on sensitive loads. Commonly known as DVR, they have a similar configuration as the SeAF. These two categories are different from each other in their control principle. This difference relies on the purpose of their application in the system.

ISSN (Print) : 2320 – 3765
ISSN (Online): 2278 – 8875

International Journal of Advanced Research in Electrical, Electronics and Instrumentation Engineering

(An ISO 3297: 2007 Certified Organization)

Website: www.ijareeie.com

Vol. 6, Issue 4, April 2017

The hybrid series active filter (HSeAF) was proposed to address the aforementioned issues with only one combination. Hypothetically, they are capable to compensate current harmonics, ensuring a power factor (PF) correction and eliminating voltage distortions at the PCC [11]. These properties make it an appropriate candidate for power quality investments. The three-phase SeAFs are well documented [13, whereas limited research works reported the single-phase applications of SeAFs in the literature. In this paper, a single-phase transformer less HSeAF is proposed and capable of cleaning up the grid-side connection bus bar from current harmonics generated by a nonlinear load [15]. With a smaller rating up to 10%, it could easily replace the shunt active filter [16]. Furthermore, it could restore a sinusoidal voltage at the load PCC.

The advantage of the proposed configuration is that nonlinear harmonic voltage and current producing loads could be effectively compensated. The transformer less hybrid series active filter (THSeAF) is an alternative option to conventional power transferring converters in distributed generation systems with high penetration of renewable energy sources, where each phase can be controlled separately and could be operated independently of other phases [17]. This paper shows that the separation of a three-phase converter into single-phase H bridge converters has allowed the elimination of the costly.

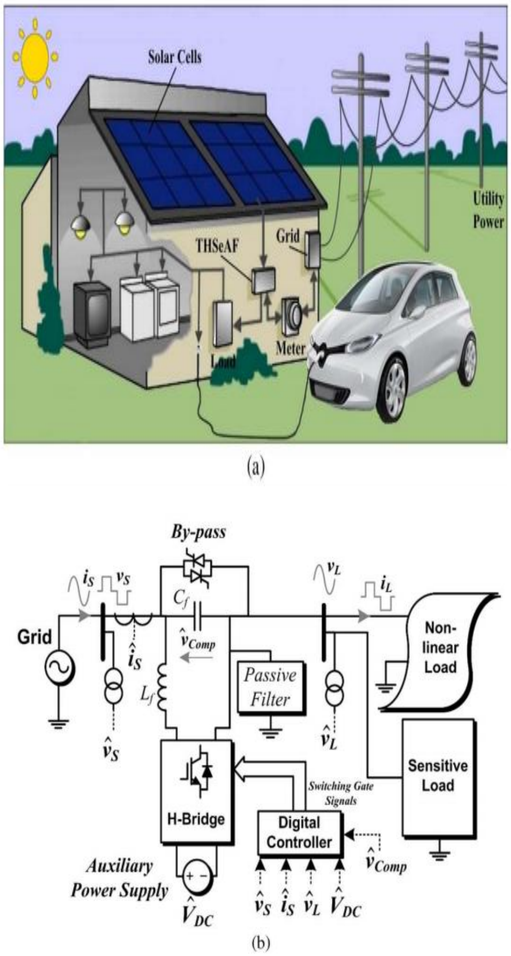

Fig.1. (a) Schematic of a single-phase smart load with the compensator installation. (b) Electrical diagram of the THSeAF in a single-phase utility.

ISSN (Print) : 2320 – 3765
ISSN (Online): 2278 – 8875

International Journal of Advanced Research in Electrical, Electronics and Instrumentation Engineering

(An ISO 3297: 2007 Certified Organization)

Website: www.ijareeie.com

Vol. 6, Issue 4, April 2017

isolation transformer and promotes industrial application for filtering purposes. The setup has shown great ability to perform requested compensating tasks for the correction of current and voltage distortions, PF correction, and voltage restoration on the load terminal [18].

This paper is organized as follows. The system architecture is introduced in the following section. Then, the operation principle of the proposed configuration is explained. The third section is dedicated to the modelling and analysis of the control algorithm implemented in this work. The dc voltage regulation and its considerations are briefly explained, and the voltage and current harmonic detection method is explicitly described. To evaluate the configuration and the control approach, some scenarios are simulated. Experimental results performed in the laboratory are demonstrated to validate simulations. This paper is summarized with a conclusion and appendix where further mathematical developments are demonstrated.

II MODELING AND CONTROL OF THE SINGLE-PHASE THSeAF:

A. Average and Small-Signal Modelling:

Based on the average equivalent circuit of an inverter, the small-signal model of the proposed configuration can be obtained as in Fig. 4. Hereafter, *d* is the duty cycle of the upper switch during a switching period, whereas $\bar{v}$ and $\bar{i}$ denote the average values in a switching period of the voltage and current

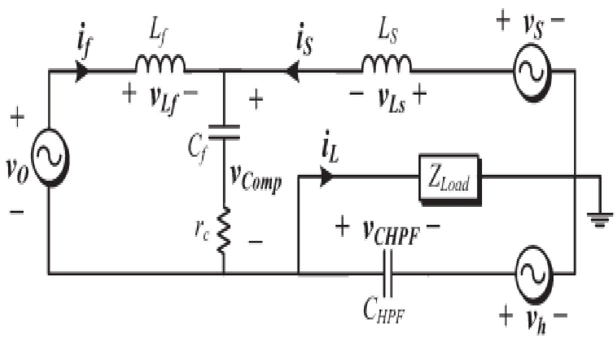

Fig.2. Small-signal model of transformerless HSeAF in series between the grid and the load.

of the same leg. The mean converter output voltage and current are expressed by (6) and (7) as follows:

$$\bar{v}_O = \underbrace{(2d-1)}V_{\mathrm{DC}} \tag{1}$$

where the $(2d - 1)$ equals to m, then

$$\bar{i}_{\mathrm{DC}} = m\bar{i}_f. \tag{2}$$

ISSN (Print) : 2320 – 3765
ISSN (Online): 2278 – 8875

International Journal of Advanced Research in Electrical, Electronics and Instrumentation Engineering

(An ISO 3297: 2007 Certified Organization)

Website: www.ijareeie.com

Vol. 6, Issue 4, April 2017

Calculating the Thevenin equivalent circuit of the harmonic current source leads to the following assumption:

$$\bar{v}_h(j\omega) = \frac{-j\bar{i}_h}{C_{HPF} \cdot \omega_h}. \tag{3}$$

If the harmonic frequency is high enough, it is possible to assume that there will be no voltage harmonics across the load. The state-space small-signal ac model could be derived by a linearized perturbation of the averaged model as follows:

$$\dot{x} = Ax + Bu. \tag{4}$$

Hence, we obtain

$$\frac{d}{dt}\begin{bmatrix} \bar{v}_{Cf} \\ \bar{v}_{CHPF} \\ \bar{i}_S \\ \bar{i}_f \\ \bar{i}_L \end{bmatrix} = \begin{bmatrix} 0 & 0 & \frac{1}{C_f} & \frac{1}{C_f} & 0 \\ 0 & 0 & \frac{1}{C_{HPF}} & 0 & -1/C_{HPF} \\ -1/L_S & -1/L_S & -r_c/L_S & -r_c/L_S & 0 \\ -1/L_f & 0 & -r_c/L_f & -r_c/L_f & 0 \\ 0 & \frac{1}{L_L} & 0 & 0 & -R_L/L_L \end{bmatrix} \times \begin{bmatrix} \bar{v}_{Cf} \\ \bar{v}_{CHPF} \\ \bar{i}_S \\ \bar{i}_f \\ \bar{i}_L \end{bmatrix} + \begin{bmatrix} 0 & 0 & 0 \\ 0 & 0 & 0 \\ \frac{1}{L_S} & 0 & \frac{1}{L_S} \\ 0 & \frac{m}{L_f} & 0 \\ 0 & 0 & -1/L_L \end{bmatrix} \times \begin{bmatrix} \bar{v}_S \\ V_{\mathrm{DC}} \\ \bar{v}_h \end{bmatrix}. \quad (1 \tag{5}$$

Moreover, the output vector is

$$y = Cx + Du \tag{6}$$

Or

$$\begin{bmatrix} \bar{v}_{\mathrm{comp}} \\ \bar{v}_L \end{bmatrix} = \begin{bmatrix} 1 & 0 & r_c & r_c & 0 \\ 0 & 1 & 0 & 0 & 0 \end{bmatrix} \times \begin{bmatrix} \bar{v}_{Cf} \\ \bar{v}_{CHPF} \\ \bar{i}_S \\ \bar{i}_f \\ \bar{i}_L \end{bmatrix} + \begin{bmatrix} 0 & 0 & 0 \\ 0 & 0 & -1 \end{bmatrix} \times \begin{bmatrix} \bar{v}_S \\ V_{\mathrm{DC}} \\ \bar{v}_h \end{bmatrix}. \tag{7}$$

The transfer function of the compensating voltage versus the load voltage, *TV _CL*(s), and the source current, *TCI* (s), are developed in the Appendix. Meanwhile, to control the active

ISSN (Print) : 2320 – 3765
ISSN (Online): 2278 – 8875

International Journal of Advanced Research in Electrical, Electronics and Instrumentation Engineering

(An ISO 3297: 2007 Certified Organization)

Website: www.ijareeie.com

Vol. 6, Issue 4, April 2017

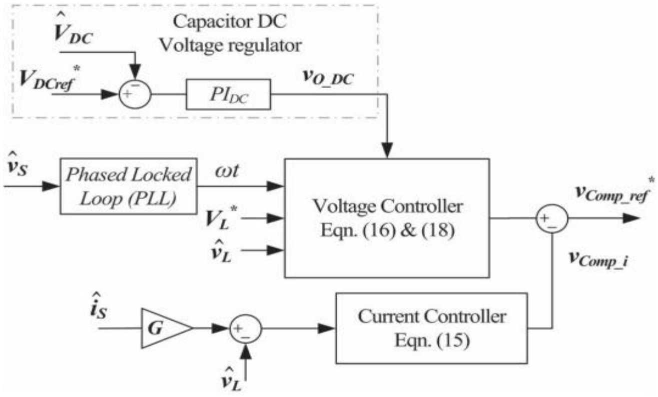

Fig.3. Control system scheme of the active part.

part independently, the derived transfer function should be autonomous from the grid configuration. The transfer function *TV m* presents the relation between the output voltages of the converter versus the duty cycle of the first leg converter's upper switch

$$T_V(s) = \frac{V_{comp}}{V_0} = \frac{r_C C_f s + 1}{L_f C_f s^2 + r_C C_f s + 1} \tag{8}$$

$$T_{Vm}(s) = \frac{V_{comp}}{m} = V_{DC} \cdot T_V(s). \tag{9}$$

The further detailed derivation of steady-state transfer functions is described .

A dc auxiliary source should be employed to maintain an adequate supply on the load terminals. During the sag or swell conditions, it should absorb or inject power to keep the voltage magnitude at the load terminals within a specified margin. However, if the compensation of sags and swells is less imperative, a capacitor could be deployed. Consequently, the dc-link voltage across the capacitor should be regulated as demonstrated

B. Voltage and Current Harmonic Detection:

The outer-loop controller is used where a capacitor replaces the dc auxiliary source. This control strategy is well explained in the previous section. The inner-loop control strategy is based on an indirect control principle. A fast Fourier transformation was used to extract the magnitude of the fundamental and its phase degree from current harmonics. The control gain ***G*** representing the impedance of the source for current harmonics has a sufficient level to clean the grid from current harmonics fed through the nonlinear load.

The second proportional integrator (PI) controller used in the outer loop was to enhance the effectiveness of the controller when regulating the dc bus. Thus, a more accurate and faster transient response was achieved without compromising the compensation behavior of the system. According to the theory, the gain ***G*** should be kept in a suitable level, preventing the harmonics from flowing into the grid [22], [24]. As previously discussed, for a more precise

ISSN (Print) : 2320 – 3765
ISSN (Online): 2278 – 8875

International Journal of Advanced Research in Electrical, Electronics and Instrumentation Engineering

(An ISO 3297: 2007 Certified Organization)

Website: www.ijareeie.com

Vol. 6, Issue 4, April 2017

compensation of current harmonics, the voltage harmonics should also be considered. The compensating voltage for current harmonic compensation is obtained from

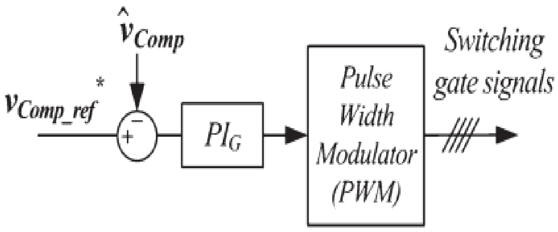

Fig.4. Block diagram of THSeAF and PI controller.

$$v_{\text{comp\_}i}(t) = \left(-G\hat{i}_S + \hat{v}_L\right) - \left[\left|-G i_{S1} + v_{L1}\right| \cdot \sin(\omega_S t - \theta)\right]. \quad \textbf{(10)}$$

Hereby, as voltage distortion at the load terminals is not desired, the voltage sag and swell should also be investigated in the inner loop. The closed-loop equation allows to indirectly maintain the voltage magnitude at the load side equal to *V* ∗ *L* as a predefined value, within acceptable margins

$$v_{\text{comp\_}v} = \hat{v}_L - V_L^* \sin(\omega_S t). \quad \textbf{(11)}$$

The entire control scheme for the THSeAF was used and implemented in MATLAB/Simulink for real-time simulations and the calculation of the compensating voltage. The real-time toolbox of dSPACE was used for compilation and execution on the dsp-1103 control board. The source and load voltages, together with the source current, are considered as system input signals. According to Srianthumrong *et al.* [25], an indirect control increases the stability of the system. The source current harmonics are obtained by extracting the fundamental component from the source current

$$v^*_{\text{com\_ref}} = v_{\text{comp\_}v} - v_{\text{comp\_}i} + v_{\text{DC\_}ref} \quad \textbf{(12)}$$

$$v_{\text{DC\_}ref}(t) = V_{O\_\text{DC}} \cdot \sin(\omega_S t). \quad \textbf{(13)}$$

A phase-locked loop was used to obtain the reference angular frequency (ωs). Accordingly, the extracted current harmonic contains a fundamental component synchronized with the source voltage in order to correct the PF. This current represents the reactive power of the load. The gain *G* representing the resistance for harmonics converts current into a relative voltage. The generated reference voltage *v*comp_*i* required to clean the source current from harmonics is described.

According to the presented detection algorithm, the compensated reference voltage *v*Comp ∗ _ref is calculated. Thereafter, the reference signal is compared with the measured output voltage and applied to a PI controller to generate the corresponding gate signals as in Fig. 4

ISSN (Print) : 2320 – 3765
ISSN (Online): 2278 – 8875

International Journal of Advanced Research in Electrical, Electronics and Instrumentation Engineering

(An ISO 3297: 2007 Certified Organization)

Website: www.ijareeie.com

Vol. 6, Issue 4, April 2017

C. Stability Analysis for Voltage and Current Harmonics:

The stability of the configuration is mainly affected by the introduced delay of a digital controller. This section studies the impact of the delay first on the inclusive compensated system according to works cited in the literature. Thereafter, their effect on the active compensator is separated from the grid. Using purely inductive source impedance and Kirchhoff's law for harmonic frequency components, (19) is derived. The delay time of the digital controller, large gain *G*, and the

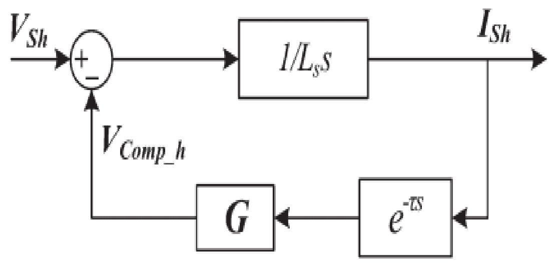

Fig.5. Control diagram of the system with delay.

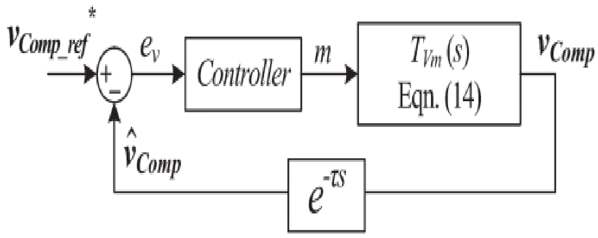

Fig.6. Closed-loop control diagram of the active filter with a constant delay time τ.

high stiffness of the system seriously affect the stability of the closed-loop controlled system
A system with a typical source inductance Ls of 250 μH and a delay of 40 μs is considered stable according to (22) when the gain ***G*** is smaller than 10Ω. Experimental results confirm the stability of the system presented in this paper. Moreover, the influence of the delay on the control algorithm should also be investigated. According to the transfer functions (13) and (14), the control of the active part is affected by the delay introduce by the digital controller. Thus, assuming an ideal switching characteristic for the IGBTs, the closed-loop system for the active part controller is shown in Fig. 8.

II. BLDC MOTOR

BLDC engine comprises of the perpetual magnet rotor and an injury stator. The brushless engines are controlled utilizing a three stage inverter. The engine obliges a rotor position sensor for beginning and for giving legitimate compensation arrangement to turn on the force gadgets in the inverter extension. In light of the rotor position, the force gadgets are commutated consecutively every 60 degrees. The electronic compensation takes out the issues connected with the brush and the commutator plan, in particular starting and destroying of the commutator brush course of action, along these lines, making a BLDC engine more rough contrasted with a dc engine. Fig.4 demonstrates the stator of the BLDC engine and fig.11 shows rotor magnet plans.

ISSN (Print) : 2320 – 3765
ISSN (Online): 2278 – 8875

International Journal of Advanced Research in Electrical, Electronics and Instrumentation Engineering

(An ISO 3297: 2007 Certified Organization)

Website: www.ijareeie.com

Vol. 6, Issue 4, April 2017

Fig.7. BLDC motor stator construction

Fig.8. BLDC motor Rotor construction.

The brush less dc engine comprise of four fundamental parts Power converter, changeless magnet brushless DC Motor (BLDCM), sensors and control calculation. The force converter changes power from the source to the BLDCM which thus changes over electrical vitality to mechanical vitality. One of the remarkable highlights of the brush less dc engine is the rotor position sensors, in view of the rotor position and order signals which may be a torque charge, voltage summon, rate order etc; the control calculation s focus the entryway sign to every semiconductor in the force electronic converter.

The structure of the control calculations decides the sort of the brush less dc engine of which there are two principle classes voltage source based drives and current source based drives. Both voltage source and current source based commute utilized for perpetual magnet brushless DC machine. The back emf waveform of the engine is demonstrated in the fig. 6. Be that as it may, machine with a non sinusoidal back emf brings about diminishment in the inverter size and lessens misfortunes for the same influence level.

ISSN (Print) : 2320 – 3765
ISSN (Online): 2278 – 8875

International Journal of Advanced Research in Electrical, Electronics and Instrumentation Engineering

(An ISO 3297: 2007 Certified Organization)

Website: www.ijareeie.com

Vol. 6, Issue 4, April 2017

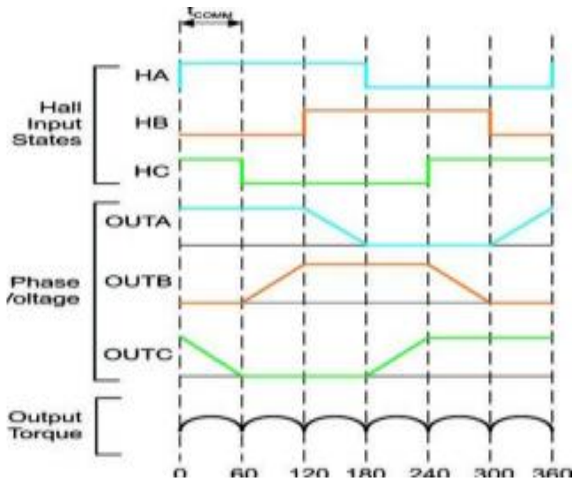

Fig.9. Hall signals & Stator voltages.

IV SIMULATION RESULTS

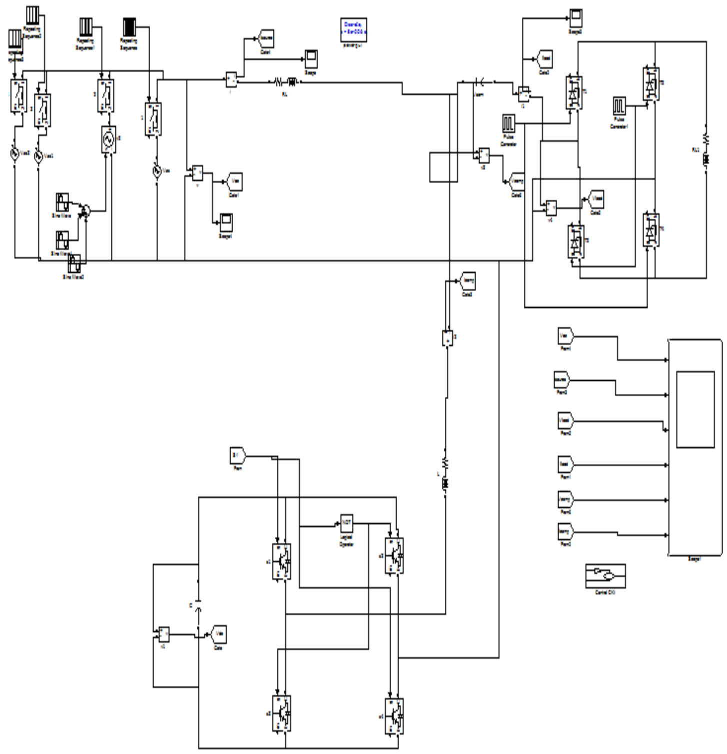

Fig .10 Matlab/Simulink conventional method circuit of a single-phase smart load with the compensator installation.

ISSN (Print) : 2320 – 3765
ISSN (Online): 2278 – 8875

International Journal of Advanced Research in Electrical, Electronics and Instrumentation Engineering

(An ISO 3297: 2007 Certified Organization)

Website: www.ijareeie.com

Vol. 6, Issue 4, April 2017

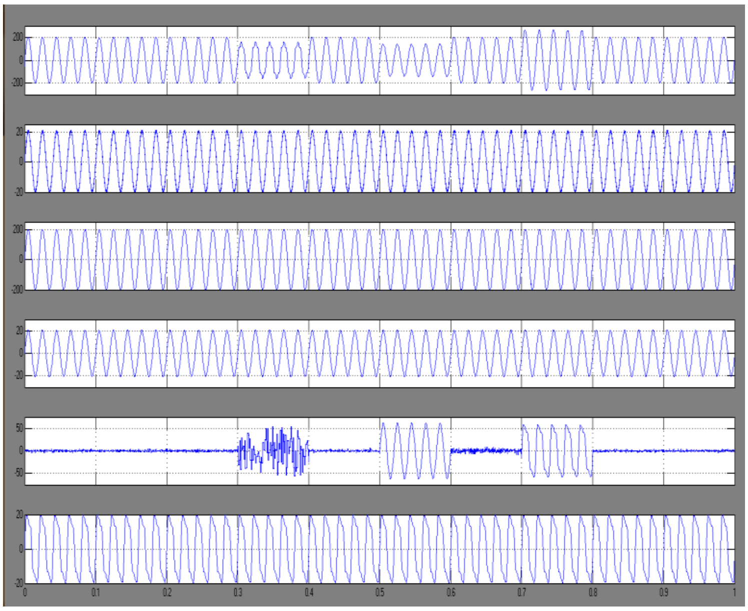

Fig 11 Simulation of the system with the THSeAF compensating current harmonics and voltage regulation. (a) Source voltage *vS*, (b)sourcecurrent *iS*, (c) load voltage *vL*, (d) load current *iL*, (e) active-filter voltage *V*Comp, and (f) harmonics current of the passive filter *i*PF

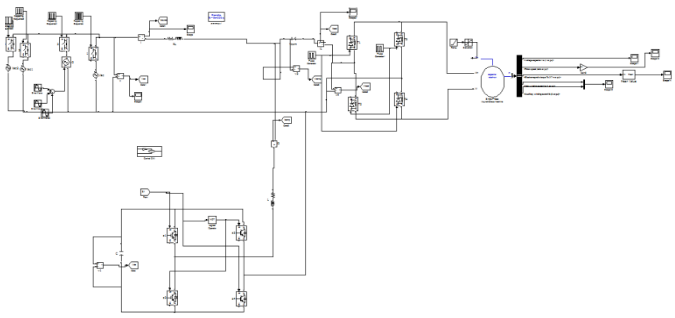

Fig 12 Matlab/Simulink proposed method circuit of a single-phase smart load with the compensator installation with BLDC motor drive

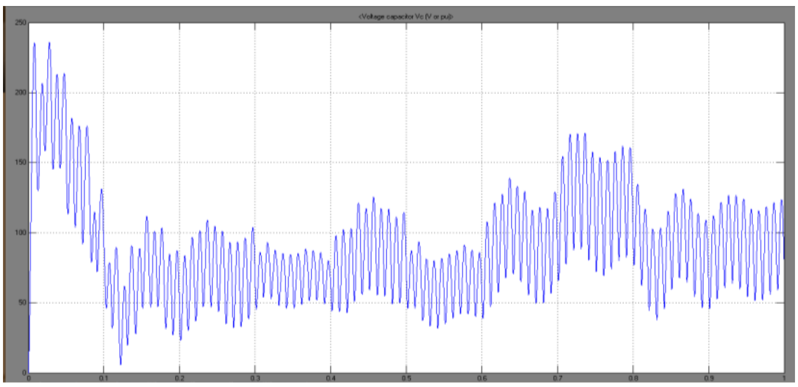

Fig 13 simulation wave form of BLDC motor drive in capacitor voltage

ISSN (Print) : 2320 – 3765
ISSN (Online): 2278 – 8875

International Journal of Advanced Research in Electrical, Electronics and Instrumentation Engineering

(An ISO 3297: 2007 Certified Organization)

Website: www.ijareeie.com

Vol. 6, Issue 4, April 2017

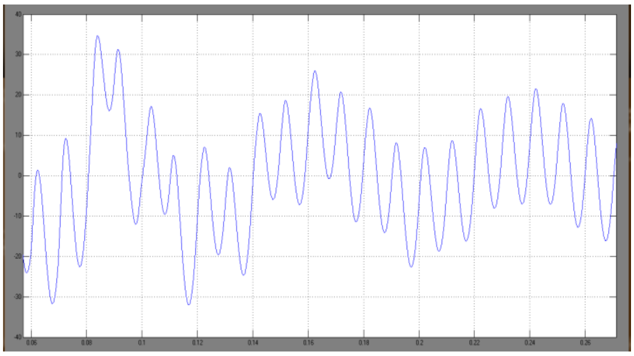

Fig 14 simulation wave form of BLDC motor drive rotor speed

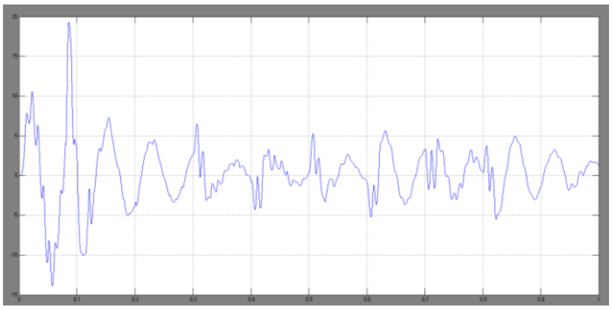

Fig 15 simulation wave form of BLDC motor drive electromagnetic torque

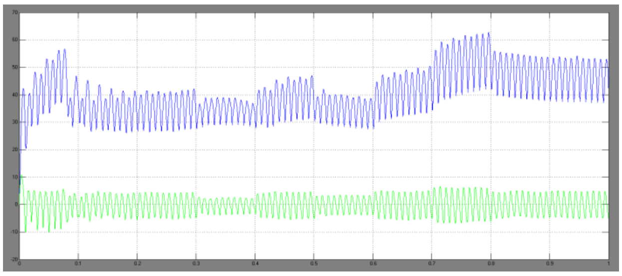

Fig 16 simulation wave form of BLDC motor drive current

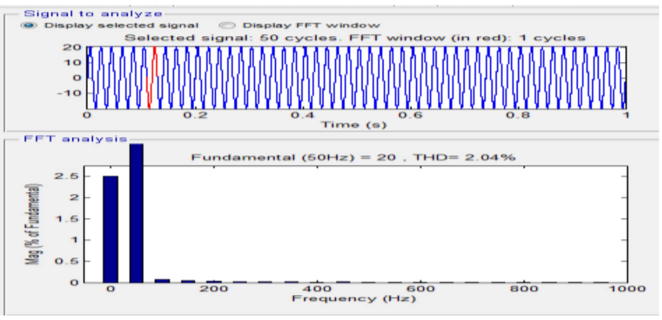

Fig 17 FFT analysis of THD =2.04%

ISSN (Print) : 2320 – 3765
ISSN (Online): 2278 – 8875

International Journal of Advanced Research in Electrical, Electronics and Instrumentation Engineering

(An ISO 3297: 2007 Certified Organization)

Website: www.ijareeie.com

Vol. 6, Issue 4, April 2017

V CONCLUSION

In this project, a transformer less HSeAF for power quality improvement was developed and tested. The paper highlighted the fact that, with the ever increase of nonlinear loads and higher exigency of the consumer for a reliable supply, concrete actions should be taken into consideration for future smart grids in order to smoothly integrate electric car battery chargers to the grid. The key novelty of the proposed solution is that the proposed configuration could improve the power quality of the system in a more general way by compensating a wide range of harmonics current, even though it can be seen that the THSeAF regulates and improves the PCC voltage. Connected to a renewable auxiliary source, the topology is able to counteract actively to the power flow in the system. This essential capability is required to ensure a consistent supply for critical loads. Behaving as high-harmonic impedance, it cleans the power system and ensures a unity PF. The theoretical modeling of the proposed configuration was investigated. The proposed transformer less configuration was simulated and experimentally validated. It was demonstrated that this active compensator responds properly to source voltage variations by providing a constant and distortion-free supply at load terminals. Furthermore, it eliminates source harmonic currents and improves the power quality of the grid without the usual bulky and costly series transformer and to analysis the BLDC motor drive

REFERENCES

[1] L. Jun-Young and C. Hyung-Jun, “6.6-kW onboard charger design using DCM PFC converter with harmonic modulation technique and two-stage dc/dc converter,” *IEEE Trans. Ind. Electron.*, vol. 61, no. 3, pp. 1243– 1252, Mar. 2014.
[2] R. Seung-Hee, K. Dong-Hee, K. Min-Jung, K. Jong-Soo, and L. ByoungKuk, “Adjustable frequency duty-cycle hybrid control strategy for fullbridge series resonant converters in electric vehicle chargers,” *IEEE Trans. Ind. Electron.*, vol. 61, no. 10, pp. 5354–5362, Oct. 2014.
[3] P. T. Staats, W. M. Grady, A. Arapostathis, and R. S. Thallam, “A statistical analysis of the effect of electric vehicle battery charging on distribution system harmonic voltages,” *IEEE Trans. Power Del.*, vol. 13, no. 2, pp. 640–646, Apr. 1998.
[4] A. Kuperman, U. Levy, J. Goren, A. Zafransky, and A. Savernin, “Battery charger for electric vehicle traction battery switch station,” *IEEE Trans. Ind. Electron.*, vol. 60, no. 12, pp. 5391–5399, Dec. 2013.
[5] Z. Amjadi and S. S. Williamson, “Modeling, simulation, control of an advanced Luo converter for plug-in hybrid electric vehicle energy-storage system,” *IEEE Trans. Veh. Technol.*, vol. 60, no. 1, pp. 64–75, Jan. 2011.
[6] H. Akagi and K. Isozaki, “A hybrid active filter for a three-phase 12-pulse diode rectifier used as the front end of a medium-voltage motor drive,” *IEEE Trans. Power Del.*, vol. 27, no. 1, pp. 69–77, Jan. 2012.
[7] A. F. Zobaa, “Optimal multiobjective design of hybrid active power filters considering a distorted environment,” *IEEE Trans. Ind. Electron.*, vol. 61, no. 1, pp. 107–114, Jan. 2014.
[8] D. Sixing, L. Jinjun, and L. Jiliang, “Hybrid cascaded H-bridge converter for harmonic current compensation,” *IEEE Trans. Power Electron.*, vol. 28, no. 5, pp. 2170–2179, May 2013.
[9] M. S. Hamad, M. I. Masoud, and B. W. Williams, “Medium-voltage 12-pulse converter: Output voltage harmonic compensation using a series APF,” *IEEE Trans. Ind. Electron.*, vol. 61, no. 1, pp. 43–52, Jan. 2014.
[10] J. Liu, S. Dai, Q. Chen, and K. Tao, “Modelling and industrial application of series hybrid active power filter,” *IET Power Electron.*, vol. 6, no. 8, pp. 1707–1714, Sep. 2013.
[11] A. Javadi, H. Fortin Blanchette, and K. Al-Haddad, “An advanced control algorithm for series hybrid active filter adopting UPQC behavior,” in *Proc. 38th Annu. IEEE IECON*, Montreal, QC, Canada, 2012, pp. 5318–5323.
[12] O. S. Senturk and A. M. Hava, “Performance enhancement of the singlephase series active filter by employing the load voltage waveform reconstruction and line current sampling delay reduction methods,” *IEEE Trans. Power Electron.*, vol. 26, no. 8, pp. 2210–2220, Aug. 2011.
[13] A. Y. Goharrizi, S. H. Hosseini, M. Sabahi, and G. B. Gharehpetian, “Three-phase HFL-DVR with independently controlled phases,” *IEEE Trans. Power Electron.*, vol. 27, no. 4, pp. 1706–1718, Apr. 2012.
[14] H. Abu-Rub, M. Malinowski, and K. Al-Haddad, *Power Electronics for Renewable Energy Systems, Transportation, Industrial Applications*. Chichester, U.K.: Wiley InterScience, 2014.
[15] S. Rahmani, K. Al-Haddad, and H. Kanaan, “A comparative study of shunt hybrid and shunt active power filters for single-phase applications: Simulation and experimental validation,” *Math. Comput. Simul.*, vol. 71, no. 4–6, pp. 345–359, Jun. 19, 2006.

[16] W. R. Nogueira Santos *et al.*, “The transformerless single-phase universal active power filter for harmonic and reactive power compensation,” *IEEE Trans. Power Electron.*, vol. 29, no. 7, pp. 3563–3572, Jul. 2014.
[17] A. Javadi, H. Fortin Blanchette, and K. Al-Haddad, “A novel transformerless hybrid series active filter,” in *Proc. 38th Annu. IEEE IECON*, Montreal, QC, USA, 2012, pp. 5312–5317.
[18] H. Liqun, X. Jian, O. Hui, Z. Pengju, and Z. Kai, “High-performance indirect current control scheme for railway traction four-quadrant converters,” *IEEE Trans. Ind. Electron.*, vol. 61, no. 12, pp. 6645–6654, Dec. 2014.
[19] E. K. K. Sng, S. S. Choi, and D. M. Vilathgamuwa, “Analysis of series compensation and dc-link voltage controls of a transformerless selfcharging dynamic voltage restorer,” *IEEE Trans. Power Del.*, vol. 19, no. 3, pp. 1511–1518, Jul. 200 4.